Femtosecond X-Ray Pulse Characterization in Free-Electron Lasers Using a Cross-Correlation Technique

Y. Ding, F.-J. Decker, P. Emma, C. Feng, C. Field, J. Frisch, Z. Huang, J. Krzywinski, H. Loos, J. Welch, J. Wu, and F. Zhou

Femtosecond x-ray pulse characterization in free-electron lasers using a cross-correlation technique

Y. Ding[1], F.-J. Decker[1], P. Emma[2], C. Feng[3], C. Field[1], J. Frisch[1],
Z. Huang[1], J. Krzywinski[1], H. Loos[1], J. Welch[1], J. Wu[1], F. Zhou[1]

[1] SLAC National Accelerator Laboratory, Menlo Park, California 94025, USA
[2] Lawrence Berkeley National Laboratory, Berkeley, California 94720, USA
[3] Shanghai Institute of Applied Physics, CAS, Shanghai 201800, China

We report the first measurements of x-ray single-pulse duration and two-pulse separation at the Linac Coherent Light Source using a cross-correlation technique involving x-rays and electrons. An emittance-spoiling foil is adopted as a very simple and effective method to control the output x-ray pulse. A minimum pulse duration of about 3 femtoseconds full width at half maximum has been measured together with a controllable pulse separation (delay) between two pulses. This technique provides critical temporal diagnostics for x-ray experiments such as x-ray pump-probe studies.
PACS numbers: 41.60.Cr, 41.50.+h

PACS numbers:

The realization of x-ray free-electron lasers (FEL) has opened up vast opportunities for studying ultrafast dynamics in chemistry, biology and materials science. An important class of experiments is the time-resolved, pump-probe study, where femtosecond (fs) x-rays are expected to capture the dynamic behavior of the chemical process (see, e.g. [1]).

Good progress has been made towards the generation of femtosecond x-ray pulses at the Linac Coherent Light Source (LCLS) [2]. One method is to reduce the bunch charge and hence the bunch length (e.g., from nominal operating charge of 150-250 pC down to 20 pC). The resulting x-ray pulse is less than 10 fs [3]. In this low-charge operation mode, an external pulse such as an optical laser can be adopted as a pump. However, the synchronization jitter between the pump and probe pulses is very challenging and many efforts have been made to solve this problem (see, e.g., [4], [5], and references therein).

Another method is to use an emittance-spoiling foil (a slotted foil), which was first proposed in 2004 [6] and has been on-line at the LCLS since 2010. While the dispersed electron beam passes through a foil with a single or double slots, most of the beam emittance will be spoiled, leaving very short unspoiled time slices to produce femtosecond x-rays. The ease of operation for this technique has been very useful for many scientific experiments [7], and more importantly, the two-pulse mode from double-slot setup enables x-ray pump/x-ray probe experiments without relative timing jitter issues.

On the other hand, experimentally measuring x-ray pulse duration and two-pulse separation (delay) with a femtosecond resolution constitutes a very challenging problem. New concepts of ultrafast x-ray diagnostics have been developed recently. One of them is the terahertz-field streaking method [8], where a terahertz field generated from a specific undulator modulates the photoelectrons. By measuring the photoelectron energy

spectrum the x-ray pulse temporal structure can be reconstructed. Laser-based terahertz streaking has also been developed recently [9]. Another new method is to use a transverse deflecting cavity to measure the FEL induced time-correlated electron energy spread, from which the x-ray temporal profile can be retrieved [10]. A frequency-domain method based on x-ray spectral correlation function has also been studied recently [11].

Autocorrelation is a well known method to measure pulse length at optical frequencies. In a typical intensity autocorrelator setup, a pulse is split into two, one is variably delayed with respect to the other, and the two pulses are then recombined to pass through a nonlinear optical crystal. The final pulse energy versus the delay gives an autocorrelation trace. For x-rays in the femtosecond regime, because of the vanishing small cross sections in nonlinear processes and the lack of mirrors, temporal correlation techniques are very difficult to realize. Recently Geloni et al. proposed to measure the x-ray pulse autocorrelation function combined with a "fresh" bunch technique [12]. In this proposal, a magnetic chicane is added in the middle of the FEL undulator to wash out the microbunching of electrons generated in the first part of the undulator, and also to make an offset for an x-ray optical delay line. After the chicane, the x-ray pulse overlaps with the "fresh" electron bunch, and their relative delay is controlled by the x-ray delay line. Here the "fresh" bunch idea, which was first discussed in [13], is based on the condition that the self-amplified spontaneous emission (SASE) FEL induced electron energy loss and energy spread are still small before FEL saturation. After washing out the electron microbunching, we obtain a "fresh" bunch which has a similar beam quality as before. Thus this scheme only works in the exponential gain regime. It solves the problem of having to split x-rays by using an x-ray pulse to correlate against a "fresh" electron bunch. In this sense, we call the technique cross-
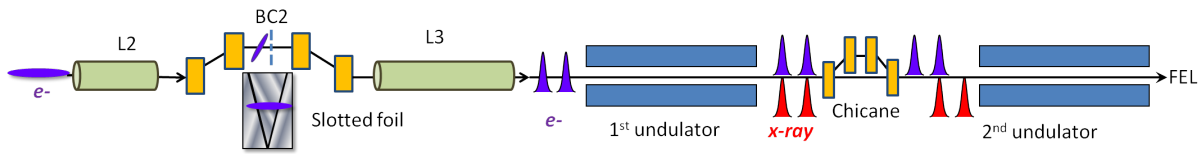
FIG. 1: A schematic layout of the emittance spoiling foil and cross-correlation configuration at the LCLS. A double-slotted foil setup is used for the illustration in this figure.

correlation instead of autocorrelation used in Ref. [12].

In this paper, we report the first measurements of single-pulse duration and two-pulse separation using a cross-correlation technique at the LCLS beamline. The single-pulse duration measurement is suggested in [12] by using only a chicane (without an optical delay line). As discussed in [12], this is a simplified setup, and as a result, only a partial correlation trace can be obtained. We then extend this technique to the two-pulse mode with a double-slotted foil. By variably delaying the electron beam, the first electron bunch crosses over the second x-ray pulse and a full correlation trace is measured, from which both the pulse separation and duration can be obtained.

Figure 1 shows the layout of the foil and the cross-correlation configuration at LCLS. The linear accelerator section (L2), before the second bunch compressor (BC2) chicane, is set at an off-crest accelerating rf phase, so the beam energy after L2 will be correlated with time. This correlation can be written as $\delta_1 = hz_1$ to the first order, where δ_1 is the electron's relative energy spread, z_1 is the electron's longitudinal coordinate, and h is a time-energy chirp generated from the off-crest acceleration. We use R_{56} [14] to describe the energy-dependent path length coefficient, or momentum compaction, of the BC2. The final bunch length coordinate (after the chicane) z_2 can be written as

$$z_2 = (1 + hR_{56})z_1 = z_1/C, \qquad (1)$$

where we defined the bunch compression factor $C = 1/(1 + hR_{56})$. Note here R_{56} is negative, and we choose L2 rf phase to have lower-energy beam at the bunch head so that the bunch is compressed after BC2. The transverse extent of the beam at the middle of the chicane, x_1, can be written in terms of the momentum dispersion, η,

$$x_1 = \eta\delta_1 = \eta hz_1. \qquad (2)$$

Here we ignored the term from the betatron component of the transverse coordinate. For a double-slotted foil with a slot separation Δx, we will get two unspoiled electron beams, and their temporal separation after the chicane can be obtained from eq. (1) and (2):

$$\Delta t = \frac{\Delta x}{\eta hCc}. \qquad (3)$$

$c = 3 \times 10^8 m/s$ is the speed of light. Similarly, we can also calculate the pulse duration from a slot with a finite width, but the uncorrelated energy spread and betatron beam size have to be included, as discussed in [15]. The main difficulty in the calculations is to know the beam chirp h. The collective effects and high order optics are also hard to include in a simple calculation.

To achieve a variable pulse duration and separation, an aluminum foil (3 μm thickness) with different slot arrays was designed. Its design of the present version includes a vertical V-shape single slot with a variable slot width (220-1580 μm), and two V-shape double slots with different slot separation at two fixed slot widths (300 and 430 μm), as shown in the bottom of Fig. 2. The choice of these slot sets were determined by the user interests, FEL performance and also the practical considerations of manufacturing.
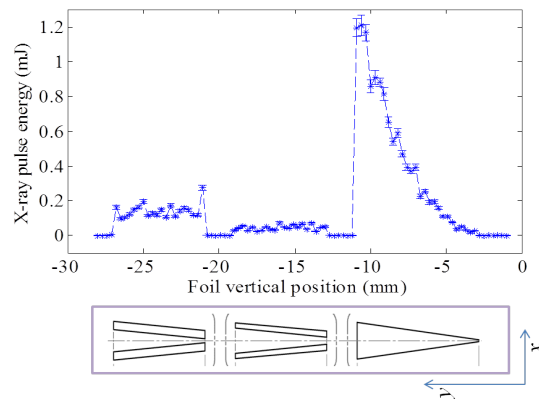
FIG. 2: Measured FEL pulse energy (blue stars) vs. foil vertical position. A motor controls the foil vertical position to have electrons pass through different slot arrays (bottom).

After the electron beam passes through the emittance-spoiling foil, one or two unspoiled time slices with good emittance will contribute to FEL lasing. We show one example of the measured FEL pulse energy versus the foil vertical position in Fig. 2. The photon energy was 1.5 keV, and the electron beam energy was 5.8 GeV with peak current of 1.5 kA. When the electron beam emittance is totally spoiled, for example, at the far right part of this figure, the FEL beam is fully suppressed. While moving the foil vertically to let the beam pass through

the narrower part of the single slot, the FEL beam intensity starts to grow. With a very narrow slit, the uncorrelated energy spread and betatron beam size dominate the output pulse length [15], and we get a nonlinear growth of the pulse energy versus the slot width. When the slot gets larger, the growth becomes linear and the pulse length is mainly determined by the slot width [15]. It is also shown that in the two double-slot areas, the measured pulse energy from each area is almost constant, while the pulse separation actually varies during the scan.

Since 2012, one LCLS undulator segment U16 (of 33 four-meter long undulator sections) has been replaced with a 3.2-m long magnetic chicane for hard x-ray self-seeding program [16]. This chicane enables the cross-correlation measurements by operating the FEL in SASE mode. It plays two roles: to wash out the FEL microbunching generated in the first part of the undulator, and to delay the electron beam with respect to the x-rays. The maximum delay from this chicane is about 40 fs with the present chicane and chamber design.
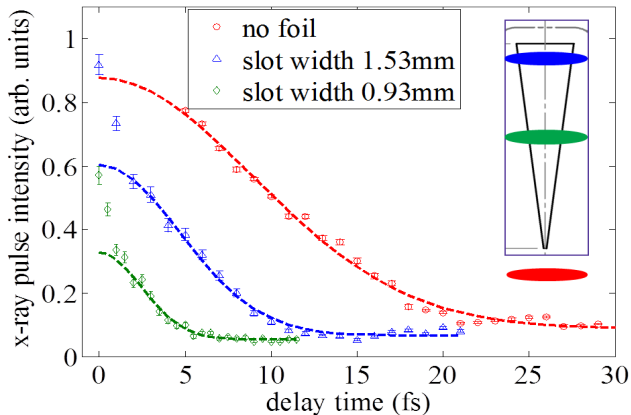
FIG. 3: Cross-correlation measurements for a single bunch: no foil (red circles), with slot width 1.53 mm (blue triangles) and with slot width 0.93 mm (green diamonds). The dashed lines show Gaussian fit results (fitting is from a minimum delay of 2 fs). With a deconvolution factor 1.5, the obtained fwhm x-ray pulse durations are 14.1 fs, 7.3 fs and 3.8 fs.

Figure 3 shows measured cross-correlation data for the single bunch mode with different slot widths. The electron beam charge was 150 pC, the peak current was 3 kA, and the energy was 13.6 GeV. The x-ray photon energy was 8.3 keV. We used 13 undulator sections for each part in this measurement. A gas detector or a YAG screen records the final x-ray pulse energy. Each data point is based on an average of 60 recorded shots. For this single bunch mode, the intensity correlation function should reach its maximum value at a relative delay $\tau = 0$ (overlapped), then it should go down with a larger delay until the x-ray pulse and the electron bunch totally missed. Therefore, during the Gaussian fitting of the data we chose a zero offset. For the data sets with foils,

the measurements were done from a zero delay, where the microbunching was not smeared out. From the fitting results we found that the fitting curves matched the data from a delay $\tau = 2$ fs, corresponding to a chicane $R_{56} = -2\tau c = -1.2$ μm. This shows the minimum value of R_{56} needed to wash out the microbunching. To estimate the full width at half maximum (fwhm) of a pulse, the fwhm of the intensity correlation curve obtained from this fitting has to be divided by a deconvolution factor, which is related to a specific pulse shape. For example, for a Gaussian-shape bunch, this deconvolution factor is $\sqrt{2}$. Fortunately the variation in the deconvolution factor for different pulse shapes is on the order of only 10% [17], and we use 1.5 in our analysis. As shown in Fig. 3, for the no-foil case, the measured fwhm pulse duration (after dividing the factor 1.5) is 14.1 fs, and for slot widths 1.53 mm and 0.93 mm, the pulse fwhm durations are 7.3 fs and 3.8 fs, respectively. Note in the no-foil case we measured a much shorter x-ray pulse than the electron bunch (electron bunch is about 50 fs full length in this example). This may indicate the FEL lasing is from the core part or substructures of the electron bunch. We have the potential to achieve much shorter x-ray pulses by using a narrower slot, but in this setup, it is hard to measure since the first 2-fs data have to be excluded due to unsmeared microbunching effect.

Figure 4 shows three cross-correlation data for the double-slotted foil setup. The photon energy was 2 keV, and the electron bunch charge was 150 pC with a peak current of 2 kA. For this double-pulse mode, the minimum pulse separation is about 10 fs, which is big enough for the chicane to wash out the microbunching and a full cross-correlation trace can be measured. In these examples, we see a clear peak of the pulse energy while scanning the delay of the electrons. This peak means that the first electron slice overlaps with the second x-ray pulse and the FEL is enhanced, which determines the pulse separation. Also the width of the peak, as discussed in the single bunch mode, gives information about the pulse duration. A Gaussian fit has been made to get the offset (separation) and the width. As illustrated in Fig.4(d), we set up two configurations (a) and (b) with different slot separation but same slot width, and use a narrower slot width in scheme (c) with its separation same as that in (a). For scheme (a) and (b), we measured the double pulse separation of 22.7 fs and 14.7 fs. Using the same deconvolution factor of 1.5, the fwhm pulse durations are 6.1 fs and 6.5 fs. In scheme (c), the measured pulse delay is 22.6 fs, which is almost the same as that measured from (a), and the fwhm pulse duration is 3 fs, about a factor 2 reduced. This shows how we can control the pulse delay and duration by choosing slot configurations.

We also performed the correlation measurements with a uniform slot separation step (using the wide double-slot array). The photon energy was 8.3 keV. The electron charge was 150 pC with a peak current of 2600 A.

FIG. 6: The measured pulse duration vs. slot separation with a same condition in Fig. (5). Triangles show the start-to-end simulation results.
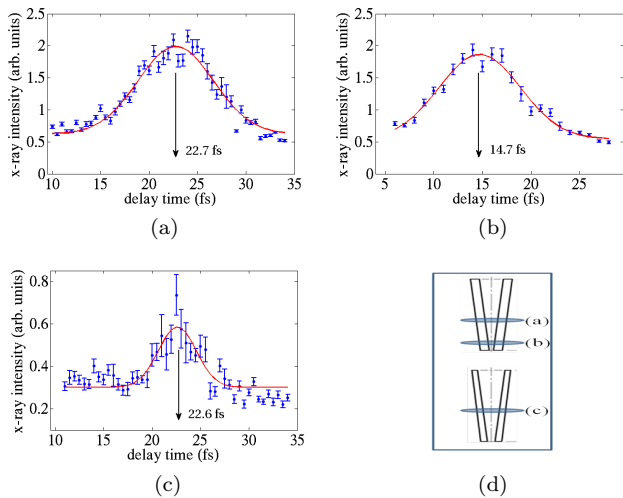
FIG. 4: The cross-correlation data (blue dots) measured at different double-slot arrays, as shown in (d). For (a) and (b), the beam was on the wide-slot area with a different slot separation. For (c), the slot separation is same as that in (a), but the slot width is narrower. Gaussian fitting results are shown with red curves.

The measured pulse delay versus slot separation is shown in Fig.5 with blue dots. The calculation results using Eq. (3) are shown with a green solid line. We see that the measured pulse delays are slightly smaller than those from calculations, and the discrepancy is getting slightly larger when the slot separation is wider.
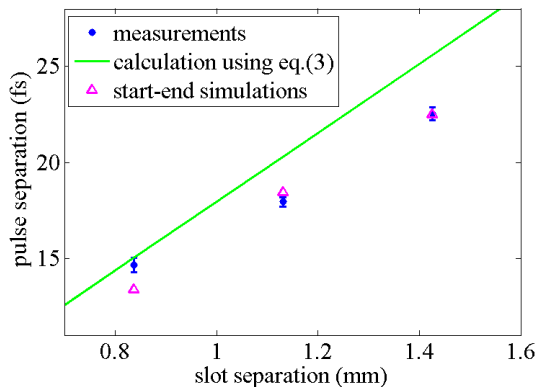
FIG. 5: The measured pulse delay vs. slot separation (blue dots) at 8.3keV photon energy, using the wide double-slot area. The calculation result using Eq. (3) is shown in a solid green line. Start-to-end Simulation results are shown with triangles.

Start-to-end simulations were carried out to understand the discrepancy. We used a 3-D space charge code IMPACT-T [18] for the injector part, and ELEGANT [19] for the main linac until the undulator entrance. For the beam-foil interaction simulations, a multiple Coulomb scattering formula was used in EL-

EGANT. The code GENESIS 1.3 [20] has been used for FEL simulations, where we get the simulated pulse delay and duration. The simulated pulse separations (triangles in Fig. 5) agree well with measurements. In the calculations using Eq. (3), a flat-top bunch shape with a linear chirp was assumed so we get a linear compression along the bunch. On the other hand, in the real machine, due to the longitudinal wake fields from the rf structure, a nonlinear chirp is formed and a double-horn temporal profile is generated after compression [21]. The local compression factor along the bunch longitudinal position is variable, with a larger compression when it is off center. This may explain the discrepancy between the simple calculation and the measurements/simulations.

At the same time, we measured the pulse duration at the different separations (blue dots in Fig. 6), and the start-to-end simulation results are shown with triangles (about 3.2 fs fwhm). They agree reasonably well. Based on a calculation similar to Eq. (3) but including the uncorrelated energy spread and emittance effects [15], the unspoiled electron bunch length is about 5.5 fs fwhm. This shows the actual pulse length is shorter than that from a simple calculation in which the high order chirp and collective effects are not included.

Note for this cross-correlation measurement, as discussed earlier, the FEL has to operate in the exponential gain regime. Compared with a regular operation in the saturation regime, the measured pulse length from this technique can be shorter when the beam shape is not uniform. In the start-to-end simulations, we set up a longer undulator to reach FEL saturation and then check the x-ray pulse evolution. We found the x-ray pulse duration lengthens about 30% (from 3.2 fs to 4.2 fs fwhm) after reaching full saturation. However, the pulse separation stays the same at different operating regimes.

In summary, femtosecond x-ray pulses with a controllable delay can be generated at LCLS using an emittance-spoiling foil. With a chicane in the middle of the un-

dulator to generate a "fresh" bunch, a cross-correlation technique for characterizing these x-ray pulses was successfully demonstrated and has been available on-line for x-ray experiments.

[1] A. H. Zewail, J. Phys. Chem. A **104**, 5660 (2000).

[2] P. Emma *et al.*, Nat. Photon. **4**, 641 (2010).

[3] Y. Ding *et al.*, Phys. Rev. Lett, **102**, 254801 (2009).

[4] F. Tavella *et al.*, Nat. Photon. **5**, 162 (2011).

[5] M. R. Bionta *et al.*, Optics Express, **19**, 21885 (2011).

[6] P. Emma *et al.*, Phys. Rev. Lett., **92**, 074801 (2004).

[7] For example, S. Schorb *et al.*, Phys. Rev. Lett., **108**, 233401 (2012).

[8] U. Frühling *et al.*, Nat. Photon. **3**, 523 (2011).

[9] A. Cavalieri *et al.*, to be published.

[10] Y. Ding *et al.*, Pys. Rev. ST Accel. Beams **14**, 120701 (2011).

[11] A. A. Lutman it et al., Pys. Rev. ST Accel. Beams **15**, 030705 (2012).

[12] G. Geloni, V. Kocharyan, and E. Saldin, *ultrafast x-ray pulse measurement method*, DESY 10-008.

[13] I. Ben-Zvi *et al.*, Nucl. Instrum. Methods A **318**, 726 (1992).

[14] A. W. Chao and M. Tigner, " Handbok of Accelerator Physics and Engineering", page 66, World Scientific Publishing Co. Pte. Ltd (2006).

[15] P. Emma, Z. Huang, and M. Borland, Proceedings of FEL 2004, Trieste, Italy.

[16] J. Amann *et al.*, Nature Photon., **6**, 693 (2012).

[17] J-C. Diels and W. Rudolph, "Ultrashort Laser Pulse Phenomena", page 477, Academic Press second edition (2006).

[18] J. Qiang *et al.*, Phys. Rev. ST Accel. Beams **9**, 044204 (2006).

[19] M. Borland, *Elegant*, Advanced Photon Source LS-287, 2000.

[20] S. Reiche, Nucl. Instrum. Methods A **429**, 243 (1999).

[21] J. Arthur *et al.*, Linac Coherence Light Source (LCLS) Conceptual Design Report, No. SLAC-R-593, Stanford, 2002.